pH Stability of HLA-DR4 Complexes with Antigenic Peptides[†]

Michael P. Belmares,[‡] Joshua D. Rabinowitz,[‡] Wendy Liu,[§] Elizabeth D. Mellins,[§] and Harden M. McConnell*,[‡]

*Department of Chemistry, Stanford University, Stanford, California 94305, and
Department of Pediatrics, Stanford University Medical School, Stanford, California 94305*

Received July 5, 2000

ABSTRACT: Complexes between antigenic peptides and class II proteins of the major histocompatibility complex (MHC) trigger cellular immune responses. These complexes usually dissociate more rapidly at mildly acidic pH, where they are formed intracellularly, as compared to neutral pH, where they function at the cell surface. This paper describes the pH dependence of the dissociation kinetics of complexes between MHC proteins and antigenic peptides containing aspartic and glutamic acid residues. Some of these complexes show an unusual pH dependence, dissociating much more rapidly at pH 7 than at pH 5.3. This occurs when the carboxylate group of the aspartic or glutamic acid residue is located in a neutral pocket of the protein. In contrast, solvent-exposed carboxylate groups or carboxylate groups buried in pockets where they form salt bridges with the protein do not show this unusual pH dependence. The kinetic data having the unusual pH dependence conform closely to a model in which there is a rapid reversible equilibration between a less stable deprotonated complex and a more stable protonated complex. In this model, the pK_a of the protonation reaction for the partially buried peptide carboxylate group ranges from 7.7 to 8.3, reflecting the strongly basic conditions required for deprotonation. One of the few peptide/ MHC complexes demonstrated to play a role in autoimmunity in humans contains a buried peptide carboxylate and shows this unusual pH dependence. The relevance of this finding to understanding the chemical basis of autoimmunity is briefly discussed.

The activation of helper T lymphocytes (T cells) is a critical step in immune response. Helper T cells are triggered by molecular complexes of antigenic peptides and class II major histocompatibility complex proteins (MHC)[1] presented on the surface of specialized antigen presenting cells (*1*). MHC II molecules are α,β-heterodimeric transmembrane glycoproteins that bind peptides in an extended polyproline type II helix conformation. The structure is stabilized by hydrogen bonds between the peptide backbone and the MHC II protein as well as interactions between specific peptide side chains and pockets on the protein surface (*1−5*).

Peptide/MHC complexes are typically formed in acidic endosomal compartments, where newly synthesized MHC II proteins converge with peptides formed by proteolysis of endocytosed antigens (*1*). These endosomal compartments often contain an enzyme, HLA-DM, that accelerates peptide/ MHC complex dissociation and thus enriches the pool of complexes for those with greater stability at acidic pH (*6− 9*). Peptide/MHC complexes then exit the endosomal compartment and move to the cell surface for presentation to helper T cells. Consistent with this mechanism for antigen presentation, the peptide fragments that are most effective at eliciting an immune response (immunodominant peptides) generally form complexes with MHC II that are stable for hours at both mildly acidic (endosomal) and neutral (cell surface) pH (*10*).

It has been previously found that the great majority of peptide/MHC complexes are slightly to moderately more stable at neutral than mildly acidic pH (*11−13*). This finding is consistent with the idea that endosomal antigen presentation is designed in part to ensure that cell surface peptide/ MHC complexes are stable targets for T cell recognition. In fact, it has been previously proposed that peptide/MHC complexes that are short-lived at neutral pH may sometimes play a role in autoimmune disease (*14−16*).

In contrast to the vast majority of peptide/MHC complexes that dissociate at least as rapidly at neutral as at mildly acidic pH, we and our collaborators have recently identified one peptide/MHC complex that dissociates much more rapidly at neutral than at mildly acidic pH (an "unusual" pH dependence). This peptide/MHC complex involves the MHC protein HLA-DR4*0401, which is genetically linked to

[1] Abbreviations: CII, human collagen II; DR*04, refers to all HLA-DR4*04 alleles; f, fluorescein; Hb, hemoglobin; HCgp-39, human cartilage glycoprotein 39; HCgp-39 f327−337, HCgp-39 fluorescein-labeled wild-type peptide; f-peptide, fluorescein-labeled peptide; Ii CLIP, human invariant chain; MHC, major histocompatability complex; HEPES, *N*-(hydroxyethyl)piperazine-*N'*-2-ethanesulfonic acid; HLA-DM, human leukocyte antigen DM; MBP, myelin basic protein; MES, 2-(*N*-morpholino)ethanesulfonic acid; PBS, phosphate-buffered saline consisting of 10 mM phosphate and 150 mM NaCl (pH 7.0); PBS/ citrate pH 5.3 buffer, 9:1 PBS at pH 7.0 and 1 M sodium citrate at pH 4.8 by volume; PV, *Pemphigus vulgaris*; RA, rheumatoid arthritis; SEB, superantigen; TFA, trifluoroacetic acid. Single letter abbreviations for amino acids used: A, Ala; C, Cys; D, Asp; E, Glu; F, Phe; G, Gly; H, His; I, Ile; K, Lys; M, Met; N, Asn; P, Pro; Q, Gln; R, Arg; S, Ser; T, Thr; V, Val; W, Trp; Y, Tyr.

rheumatoid arthritis (RA) susceptibility, and a peptide from a candidate rheumatoid arthritis autoantigen, human cartilage glycoprotein 39 (HCgp-39) residues 327−337 (*17−19*). A prominent structural feature of the HCgp-39 327−337 peptide is that it contains three acidic side chains: two aspartic acids and one glutamic acid.

In this paper, we show that the unusual pH dependence of HLA-DR4*0401/HCgp-39 327−337 complex dissociation is largely due to one specific aspartic acid residue whose carboxylate group is buried in a neutral pocket on the protein surface. Motivated by this finding, we examine systematically the relationship between acidic peptide side chains and the pH dependence of peptide/MHC complex stability. A quantitative model accounts for the kinetic results and shows the effect of pocket burial on the pK_a of the carboxylate group. Finally, we examine one of the desmoglein 3 peptide/HLA-DR4*0402 complexes whose role in autoimmunity in humans (*Pemphigus vulgaris*) has been demonstrated (*20*). This peptide/MHC complex also dissociates much more rapidly at neutral than at mildly acidic pH due to a peptide carboxylate that is buried in a neutral protein pocket.

MATERIALS AND METHODS

Expression and Purification of Recombinant Soluble HLA-DR4 Molecules. Soluble HLA-DR4 (*0401, *0402, and *0404) molecules were isolated and purified as previously described (*6, 10*). Briefly, Schneider-2 (S2) *Drosophila melanogaster* cells were cotransfected with pRmHA-3 containing a soluble DRA*0101 insert, soluble DRB1 insert (*0401, *0402, or *0404) with epitope tag, and pUChs-Neo, using a calcium phosphate transfection kit (LTI). Transfected cells were cultured in Schneider's *Drosophila* medium containing 10% v/v FBS, 2 mM L-glutamine, and 50 μg/mL gentamycin and selected in 1.5 mg/mL active G418 (LTI). Selected cells were induced for 7 days with 1 mM $CuSO_4$, and DR expression was verified by Western blotting of tissue culture supernatants using an anti-DR antiserum (CHAMP; gift of L. Stern, MIT) and the epitope tag-specific monoclonal antibody (mAb), KT3. Cells expressing sDR*04 were cloned by limiting dilution (1 cell/well) in the presence of untransfected S2 feeder cells and 1.5 mg/mL G418. A clone with high expression was identified by Western blotting. For affinity purification, cultures were scaled up in 0.5-L spinner flasks.

The protocol for immunoaffinity purification of recombinant DR molecules was similar to that described by Gorga et al. (*21*). Briefly, the anti-DR mAb, L243, which recognizes assembled α,β dimers, was coupled to CNBr-activated Sepharose 4B (Pharmacia) using the manufacturer's protocol. PMSF (1mM final concentration) and, in some experiments, iodoacetamide (10 mM) was added to tissue culture supernatants after induction. Cell debris and insoluble material were removed by centrifugation, followed by filtration through a 0.20 μM CN membrane (Nalgene). Cleared supernatants were passed over the columns at least twice. After being washed in PBS, protein was eluted with 0.10 M Tris-HCl, pH 11.0, and neutralized immediately with 0.2 vol of 2 M Tris-HCl, pH 6.8. Protein-containing fractions, determined by absorbance at 280 nm, were pooled and concentrated by centrifugal ultrafiltration (Centricon-30, Amicon). Eluates were analyzed for purity by SDS−PAGE

and Coomassie Blue staining; DR α and β chain bands comprised greater or equal to 85% of total protein. Heterodimeric assembly was checked by native PAGE performed as described (*22*). Soluble DR protein (sDR) (*6*) was quantitated using the Bradford assay (Bio-Rad).

Synthesis and Purification of Peptides. Peptides were synthesized with standard FMOC chemistry on an Applied Biosystems 431A peptide synthesizer (Applied Biosystems, Foster City, CA). When indicated, the peptide resins were labeled overnight at the free N-termini with 5-fold molar excess 5- (and 6-)carboxyfluorescein succinimidyl ester (Molecular Probes) in dimethyl sulfoxide and a catalytic amount of diisopropylethylamine. Acetylation of resins was done with 10-fold molar excess acetic anhydride and pyridine in dimethyl formamide for 45 min. Resin cleaving was done for ∼3 h at room temperature with trifluoroacetic acid in the presence of ∼5% 1,2-ethanedithiol and 5% thioanisole as described elsewhere (*23*). The peptides were purified by HPLC (reversed-phase chromatography) and checked for identity and purity by mass spectrometry. The following names and sequences of the peptides were used in this study: HCgp-39 f327−337 (f-GYDDQESVKSK, f = fluorescein), HCgp-39 f327−337 D329N (f-GYNDQESVKSK), HCgp-39 f327−337 D330N (f-GYDNQESVKSK), HCgp-39 f327−337 E332Q (f-GYDDQQSVKSK), HCgp-39 f327−337 D330N S333D (f-GYDNQEDVKSK), HCgp-39 f327−337 Q331E (f-GYDDEESVKSK), HCgp-39 298−313 C300A (EIADFLRGATVHRTLG), CII f261−272 (f-AGFKGEQG-PKGE, CII = human collagen II, C-terminus amidated), CII f261−272 E266Q (f-AGFKGQQGPKGE, C-terminus amidated), CII f261−272 G265S G268S G271S (f-AGFKSE-QSPKSE, C-terminus amidated), murine fIi CLIP 85−99 P95E (f-KPVSQMRMATELLMR, Ii CLIP = invariant chain), murine fIi CLIP 85−99 (f-KPVSQMRMATPLLMR), murine fIi CLIP 85−99 M98E (f-KPVSQMRMATPLLER), murine fIi CLIP 85−99 V87A P95E M98E (f-KPASQM-RMATELLER), mHb f64−76 V67W E73D (f-GKKWI-TAFNDGLK, Hb = hemoglobin), mHb f64−73 V67I I68V (fGKKIVTAFNEGLK), human fIi-CLIP 81−104 (LPKPP-KPVSKMRMATPLLMQALPM), human desmoglein 3 f192−204 (f-SKIAFKIVSQEPA), human desmoglein 3 f192−204 E202Q (f-SKIAFKIVSQQPA), and influenza haemagglutinin (HA) 306−318 (*Ac*PKYVKQNTLKLAT, Ac = acetyl).

Preparation of Peptide/MHC II Complex. HLA-DR4*0401, *0402, and *0404 (1.7 μM) were incubated with excess peptide overnight in a 37 °C incubator at pH ∼5.3. The buffer composition at pH 5.3 was usually 9 parts by volume of PBS pH 7 buffer (PBS = 10 mM phosphate, 150 mM NaCl, and 0.02% NaN_3) to 1 part 1 M sodium citrate pH 4.8 buffer. Initial experiments using f327−337 HCgp-39 and mutants of the same peptide were done with 100 μM peptide concentration during the incubation phase with MHC II. However, it has been observed that comparable MHC II loading efficiency is achieved with ∼10−20 μM peptide concentration without affecting the dissociation kinetics results (data not shown). Therefore, most MHC II loading was done with a peptide concentration on the order of 10−20 μM.

Isolation of Peptide/MHC II Complex for Kinetic Measurements. The peptide/MHC II association solution was cooled to 4 °C. Then, the excess free peptide was separated from the complex with a small scale Bio-Rad spin column

at 4 °C. (Spin columns were packed with Sephadex G50 superfine [Pharmacia] and protein-blocked with 1% BSA /PBS solution to reduce MHC II binding to the column. Spin columns were then washed with excess PBS pH 7.0 buffer before use.) The eluted solution containing the complex was brought to a final volume of ~780 μL with PBS pH 7.0 (or PBS/citrate for experiments at pH 5.3 unless indicated otherwise). An appropriate unlabeled peptide competitor (10 μM final concentration) was also added to prevent fluorescent peptide rebinding during the dissociation kinetics. Since haemagglutinin 306−318 (Ac HA 306−318) binds well to HLA-DR4*0401, it was used as a competitor for this allele. Unlabeled HCgp-39 298−313 C300A peptide was used as a competitor for kinetic measurements in HLA-Dr4*0402 since it binds very well to this allele. Unlabeled human Ii CLIP 81−104 binds reasonably well to HLA-DR4*0404 and was used as a competitor for this allele.

The pH-dependent dissociation kinetics studies of the HCgp-39 f327−337/HLA-DR4*0401 complex (Figure 2) as well as the desmoglein 3 f192−204/HLA-DR4*0402 complex (Figure 3) were done with a HEPES/MES (H/M) buffer. The HEPES/MES (H/M) system buffers well in the pH range of 5.1−8.1 and has been previously used for studying peptide/MHC II complexes (*23*). The (H/M) buffer composition is 10 mM HEPES, 10 mM MES, 150 mM NaCl, and 0.02% NaN_3, and the pH is adjusted by adding appropriate amounts of concentrated HCl or NaOH. In these studies, the peptide/MHC II complex was isolated with a spin column preequilibrated with a HEPES/MES buffer at a given pH, and the eluted complex was brought to a final volume of ~780 μL with an H/M buffer at the same pH. An appropriate peptide competitor was also added (final concentration of 10 μM).

Dissociation Kinetics Measurements. A kinetic experiment was started by injecting a 4 °C aliquot (45 μL) of the complex solution into a 5-μm particle size HPSEC chromatography (high-performance size exclusion) column (dimensions: 7.8 mm × 30 cm, G3000SWXL TSK-GEL, Tosohaas, Montgomeryville, PA) coupled to a fluorescence detector. The size exclusion column separates the f-peptide/MHC II complex from the f-peptide released by the MHC II. The complex elutes at around 9 min, while the peptide elutes approximately 2 min later with a flow rate of 1.0 mL/min and a PBS pH 7.0 mobile phase at 25 °C. The relative amount of labeled peptide/DR*04 complex was measured as a function of time by the height of the fluorescence signal detected by a fluorimeter with excitation wavelength set at 492 nm and emmision detection set to 522 nm. Earlier studies were done with a Gilson 121 fluorimeter. However, latter studies were done with a sensitive Shimadzu RF-10AXL fluorescence detector.

The half-life of the complex ($t_{1/2}$) was generally calculated from a single-exponential fit with the Microsoft Kaleidagraf software of the normalized complex fluorescence versus time:

$$F/F_0 = A \exp(-kt)$$

where F is the complex fluorescence at time t, F_0 is the initial complex fluorescence, A is a best fit parameter approximately equal to 1, and k is the dissociation rate constant that is simply related to the half-life of the complex by

$$k = \ln 2/t_{1/2}$$

When specified in Table 1, a biphasic fit refers to

$$F/F_0 = A \exp(-k_1 t) + B \exp(-k_2 t)$$

The PBS/citrate and HEPES/MES buffer systems yield nearly identical dissociation kinetic results at pH 5.3 and pH 7.0 (data not shown) for the f327−337 HCgp-39/DR*0401 complex. The two buffer systems yield comparable results at pH 7.0 and pH 5.3 for two other complexes tested as indicated in Table 1.

In terms of sample preparation history, there was no significant incubation pH effect on the measured dissociation kinetics of these systems. Specifically, incubation of HCgp-39 f327−337 with HLA-DR4*0401 at pH 5.3 and pH 7 gives very similar dissociation kinetics at pH 7.0 (data not shown). The same observation applies to the collagen II 261−272 peptide/HLA-DR4*0401 complex.

Molecular Modeling. Modeling was done with the software package LOOK (Molecular Applications Group, Palo Alto, CA). For each peptide/MHC II complex, two structures were predicted based on two different methods. The first method involves the Homology modeling option in the software. Homology modeling in this context means that the geometrical information (backbone and side chain conformations) of a reference structure is used as a starting point for the prediction of a "relaxed" structure with a different amino acid sequence but highly conserved backbone geometry (*24, 25*). Predictions of peptide/MHC II conformations are based on a reference peptide/MHC II conformation, which usually is a crystal structure. All structure predictions in this work are based on the X-ray crystal structure of HLA-DR4*0401 MHC II and a human collagen II peptide (2SEB, the SEB fragment was removed from modeling calculation) (*2*). In the Homology method, the backbone and side chains are allowed to relax during the structure prediction process. In a second structure prediction method, the backbone is initially held fixed, while the optimum side chain packing of the peptide/MHC II complex is calculated using the CARA/MUTANT option based on a self-consistent ensemble optimization (*26−28*). After the optimum side chain packing conformation is calculated, the protein backbone is allowed to relax using the Homology modeling option. The results of the predicted structures for these two methods are referred to as Homology and CARA/Homology methods in Figure 4. In a special structure prediction case, an alternate peptide/MHC II complex conformation was generated for a hypothetical invariant chain peptide mutant (MRMATPL**E**M)/HLA-DR4*0401 complex where position 8 (shown in bold) of the invariant chain was mutated from Leu to Glu. In this procedure, the optimum side chain packing of the complex was predicted using the CARA method, followed by manual rotation of the peptide Glu residue to a trans conformation, and finally followed by Homology modeling relaxation of the whole structure (inverted solid triangle, CARA/rotate/Homology method, Figure 4).

The percent burial option in LOOK was used to calculate the burial of the carboxylate group (CO_2) of Asp or Glu peptide side chains. The burial measurements are related to the solvent accessibility of these groups (*24, 29*). The solvent probe radius used in the LOOK software package is 1.4 Å.

Table 1: Dissociation Kinetic Half-Lives of Peptide/HLA-DR4 MHC II Complexes with Peptide Carboxyl Groups at Specified MHC II Pockets[a]

peptide no.	peptide/MHC II	ionizable residue at pocket no.	mutation	$t_{1/2}$, pH 5.3 (h)	$t_{1/2}$, pH 7 (h)	pH ratio
1	fGY**DDQE**SVKSK/0401 HCgp-39 f327−337/0401	2, 3, 5	wt.	300	10	0.034
2	fGY**D**NQ**E**SVKSK/0401	2, 5	D330N	760	410	0.54
3	fGYN**DQE**SVKSK/0401	3, 5	D329N	930	78	0.084
4	fGY**DDQ**QSVKSK/0401	2, 3	E332Q	230	7.1	0.031
5	fGY**D**NQ**ED**VKSK/0401[b]	2, 5, 6	D330N S333D	860	47	0.055
6	fGY**DDEE**SVKSK/0401	2, 3, 4, 5	Q331E	920	34	0.037
7	fAGFKG**E**QGPKG**E**/0401 human CII f261−272/0401	4, 10	wt.	2.7	5.1	1.9
8	fAGFKGQQGPKG**E**/0401	10	E266Q	0.29	0.53	1.8
9	fAGFKS**E**QSPKS**E**/0401[c]	4, 10	G265S G268S G271S	720	1200	1.6
10	fAGFKS**E**QSPKS**E**/0404	4, 10	G265S G268S G271S	1.2	0.37	0.30
11	fSKIAFKIVSQ**E**PA/0402[d] desmoglein 3 f192−204/0402	9	wt.	39	3.0	0.077
12	fSKIAFKIVSQQPA/0402		E202Q	730	1200	1.7
13	fKPVSQMRMATPLLMR/0401 murine fIi CLIP 85−99/0401		wt.	2.7	11	4.1
14	fKPVSQMRMATPLL**E**R/0401	9	M98E	2.4	0.62	0.25
15	fKPVSQMRMAT**E**LLMR/0401	6	P95E	2.7	0.45	0.17
16	fKPASQMRMAT**E**LL**E**R/0401[e]	6, 9	V87A P95E M98E	2.2	0.10	0.047
17	human fIi CLIP 81−104/0402		wt.	19	56	3.0
18	fKPASQMRMAT**E**LL**E**R/0402	6, 9	V87A P95E M98E	7.2	0.070	0.0097
19	human fIi CLIP 81−104/0404		wt.	12	29	2.4
20	fKPASQMRMAT**E**LL**E**R/0404	6, 9	V87A P95E M98E	2.3	0.061	0.027
21	fGKKWITAFN**D**GLK/0401[f] hemoglobin mutant/0401	7		1.1	0.77	0.68
22	fGKKIVTAFN**E**GLK/0404 hemoglobin mutant/0404	7		13	3.0	0.23

[a] The half-lives of the complexes were calculated from a best fit to a single-exponential decay function of the normalized fluorescence decay of the complex versus time unless indicated otherwise. When appropriate, the peptide mutation(s) is specified in the fourth column. In the last column, the pH ratio is the dissociation half-life of the complex at pH 7.0 divided by the half-life of the same complex at pH 5.3. Each complex was prepared and isolated as described in Materials and Methods. Most dissociation kinetics were done with (1) PBS pH 7.0 buffer (phosphate-buffered saline containing 10 mM phosphate, 150 mM NaCl, and 0.02% NaN_3) and (2) PBS/citrate pH 5.3 buffer (9 parts PBS at pH 7.0, 1 part 1 M sodium citrate at pH 4.8, and 150 mM NaCl). When indicated, a HEPES/MES buffer system was used (1 part 20 mM HEPES, 1 part 20 mM MES, 150 mM NaCl, and 0.02% NaN_3 adjusted to pH 7.0 or pH 5.3 with concentrated acid or base). All dissociation kinetics were measured in the presence of an appropriate unlabeled peptide competitor to prevent labeled peptide rebinding to the MHC II. [b] Data using HEPES/MES buffer. For comparison, use of the PBS/citrate buffer system resulted in peptide/MHC II complex half-lives of ~1200 and 33 h at pH 5.3 and pH 7.0, respectively. [c] HEPES/ MES buffer used in this case. [d] For comparison, use of the HEPES/MES buffer resulted in peptide/MHC II complex half-lives of 42 and 4.0 h at pH 5.3 and pH 7.0, respectively. [e] Data are from a monophasic fit. At pH 5.3, a slightly better fit may be obtained by a biphasic decay function. [f] Kinetics were clearly biphasic, and the lifetimes listed correspond to the fast phase of the complex (60−80% abundant). The slower dissociating component has a half-life greater than 30 h.

RESULTS

Complexes were formed by the reaction of water-soluble recombinant forms of the class II MHC proteins HLA-DR4*0401, *0402, or *0404 and fluorescently labeled peptides. Almost all of the peptide/MHC complexes were kinetically homogeneous in that they show single-exponential dissociation kinetics. Therefore, the terms stability and half-time of dissociaton of a peptide/MHC complex are used interchangeably.

The first set of experiments performed involved the peptide/MHC complex between HLA-DR4*0401 and the HCgp-39 peptide 327−337. This complex dissociates more rapidly at pH 7.0 than at pH 5.3 (*10*). In contrast to this

earlier paper that used a longer peptide (residues 322−337), we used the core epitope to minimize the possibility of formation of isomeric complexes involving multiple binding registries. The peptide employed here, f327−337, has the sequence f-GYDDQESVKSK, where f stands for fluorescein. The P1 anchor is tyrosine. Typical dissociation curves of the complex of f327−337 and DR*0401 are given in Figure 1. These dissociation kinetics are described accurately with a single exponential, with dissociation half-times of 10 and 300 h at pH 7 and pH 5.3, respectively. These data can be accounted for by the assumption that the complex of f327−337 and 0401 is present in solution in two forms, a deprotonated form C and a protonated form CH^+. If the rate of
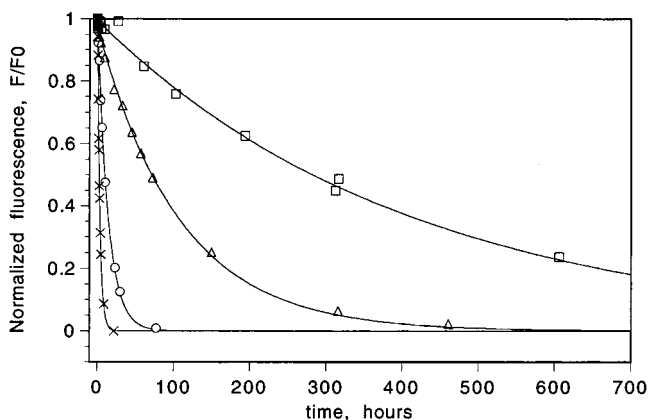
FIGURE 1: Representative dissociation kinetics. Dissociations of fluorescently labeled 327−337 human cartilage glycoprotein peptide (f327−337 HCgp-39) from HLA-DR4*0401 MHC II measured at 37 °C and pH 5.5 (squares), pH 6.2 (triangles), pH 7.0 (circles), and pH 8.0 (×). The fluorescence decay of the complex is normalized by the initial fluorescence value (t = 0). Each solid line is a fit of the data to a single-exponential decay function. The dissociation kinetics were run with a HEPES/MES buffer system (constant ionic strength) at the specified pH (HEPES/MES = 10 mM HEPES, 10 mM MES, 150 mM NaCl, and 0.02% NaN$_3$). Excess of an appropriate unlabeled peptide competitor was used to prevent labeled peptide rebinding to the MHC II.

equilibration between C and CH$^+$ is very rapid as compared to the dissociation half-times, then the dissociation half-time at any given pH is given by

$$t_{1/2}^{-1} = \frac{[H^+]K}{1 + K[H^+]}t_{1/2CH^+}^{-1} + \frac{1}{1 + K[H^+]}t_{1/2C}^{-1} \quad (1)$$

where K is the stability constant for the formation of the protonated complex:

$$K = \frac{[CH^+]}{[H^+][C]} \quad (2)$$

$t_{1/2CH^+}$ is the dissociation half-time of the protonated species, and $t_{1/2C}$ is the dissociation half-time of the nonprotonated species. The fit of the pH-dependent dissociation data to eq 1 is shown in Figure 2. In this fit, $t_{1/2C}$ is 1.6 h, $t_{1/2CH^+}$ is taken to be so large (1000 h more) that the first term in eq 1 is negligible, and K = 5.5 × 10^7. Under these conditions, the pH stability ratio, defined as

$$\rho = (t_{1/2}, pH\ 7.0)/(t_{1/2}, pH\ 5.3) \quad (3)$$

is independent of the numerical value of $t_{1/2C}$ and is equal to

$$\rho = (1 + 10^{-7}K)/(1 + 10^{-5.3}K) \quad (4)$$

For this case study, eq 4 is a good approximation for pK_a values of ∼7 or smaller using a $t_{1/2CH^+}$ of 1000 h, but pK_a values greater than 7 are underestimated under these assumptions. A pK_a of 7.1 is calculated for P3 Asp using eq 4. The best fit K value of the data to eq 1 is 5.5 × 10^7, which corresponds to a pK_a of 7.7. Therefore, the pK_a values calculated by eq 1 and estimated by eq 4 are in reasonable agreement. It will be seen that this method of estimating a stability constant using eq 4 is applicable to other peptides, provided that one complex dissociates much faster than the other and that the protonation−deprotonation reaction is fast.
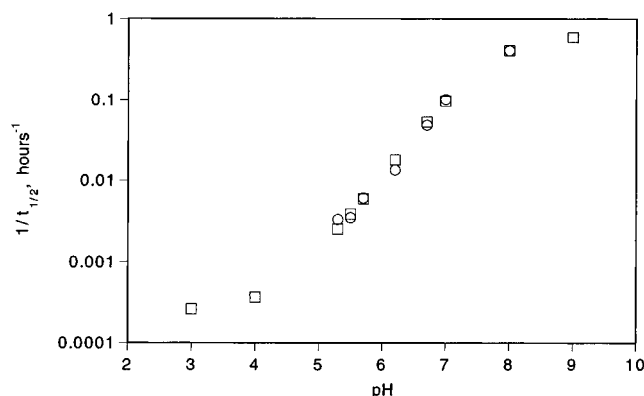

FIGURE 2: Dissociation half-times. Measured inverse dissociation half-life dependence (circles) on pH for the complex (fluorescently labeled peptide HCgp-39 327−337/HLA-DR4*0401 MHC II). The squares are a best fit of the data to a two-state model (eq 1), which assumes a protonated and deprotonated complex at a pH-dependent equilibrium where interconversion between the two states is rapid relative to the half-life of the complex. The parameters used in the fit are the half-lives of a protonated and deprotonated species with best fit values of >1000 and 1.6 h, respectively. A third parameter is an acid−base equilibrium constant (eq 2) with a best fit value equivalent to a pK_a of 7.7. The main residue responsible for this anomalous pH-dependent behavior is peptide residue 330 (Asp 330) in the peptide/MHC II complex.

The rapid protonation−deprotonation reaction is also consistent with pH jump experiments where the f327−337/DR*0401 complex was first formed by reaction of DR*0401 and f327−337 at either pH 5.3 or pH 7 at 37 °C overnight. The complex thus formed was then separated from the free peptide with a pH 7 spin column at 4 °C over 0.5 h. The pH 7 dissociation kinetics of these complexes at 37 °C are indistinguishable when formed at pH 5.3 or pH 7.0, consistent with rapid interconversion (<5 min) between the protonated and deprotonated complex (data not shown).

Table 1 summarizes a number of experiments carried out to discover the site of protonation associated with the basic pK_a for the f327−337/DR*0401 complex. It will be seen in this table that the unusual pH dependence of the dissociation half-times is almost eliminated by mutating Asp 330 to Asn. Thus, the carboxyl group of the side chain of aspartic acid at position 330 is the primary site of protonation corresponding to the pK_a of 7.7. In contrast, mutations D329N and E332Q do not remove the unusual pH dependence of the wild type.

An unusual pH ratio is not unique to peptide Asp partially buried in the P3 pocket, since the peptide D330N S333D shows that a low pH stability ratio may also be achieved by an aspartic acid side chain buried at the P6 pocket. Using eq 4, a pK_a of 6.7 is estimated for Asp at the P6 pocket for the D330N S333D 327−337/DR*0401 complex.

The autoantigenic complex formed between the truncated f-SKIAFKIVSQEPA peptide (f192−204 desmoglein 3) and HLA-DR4*0402 was also found to have a low pH stability ratio. The binding registry of this peptide places glutamic acid at the P9 pocket of DR*0402 since Ile at P1 and Lys at P4 are optimum residues for HLA-DR4*0402 (30). Substituting glutamine for glutamic acid in this peptide leads to a normal pH stability ratio as shown in Table 1. The peptide P9 glutamic acid residue is thus responsible for the unusual pH stability ratio. The pH-dependent dissociation kinetics of this complex fit within experimental error to a single-
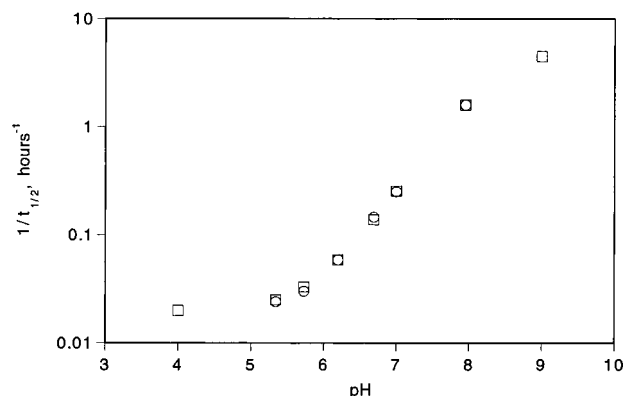
FIGURE 3: Dissociation half-times. Measured inverse half-life dependence (circles) on pH for the complex (fluorescently labeled peptide desmoglein 3 192−204/HLA-DR4*0402 MHC II). The squares are a best fit of the data to a two-state model (eq 1), which assumes a protonated and deprotonated complex at a pH-dependent equilibrium where interconversion between the two states is rapid relative to the half-life of the complex. The parameters used in the fit are the half-lives of a protonated and deprotonated species with best fit values of 51 h and 11 min, respectively. A third parameter is an acid−base equilibrium constant (eq 2) with a best fit value equivalent to a pK_a of 8.3. The main group responsible for this pH-dependent behavior was found to be peptide residue 202 (Glu 202) in the peptide/MHC II complex.

exponential decay at the measured pH values. These measurements were fit to eq 1 as shown in Figure 3, with a resulting pK_a value of 8.3 and lifetimes of 51 h and 11 min for the fully protonated and deprotonated states, respectively.

Table 1 also includes peptides with glutamic acid or aspartic acid residues at various pocket positions of DR*0401, DR*0402, and DR*0404 alleles. It is clear that the pH stability ratios are usually low for all tested pockets except P5 and P10 and to some extent P2, where carboxylates are relatively solvent exposed. Although not addressed in this study, it is expected that peptides with Asp or Glu in the relatively solvent-exposed P8 pocket bound to DR*04 MHC II will also have a normal pH stability ratio. An exception to the above rule holds for peptides with Glu at the P4 pocket of DR*0401 where there is likely to be a salt bridge (2).

Thus far, we have discussed the effects of peptides where a single buried carboxylate leads to a low pH stability ratio of the peptide/MHC II complex. In addition, the effect of two buried ionizable peptide residues on the pH ratio of the complex was measured for a CLIP peptide with a P6 glutamate and P9 glutamate bound to three DR*04 alleles. The pH ratios of these complexes are lower than those formed with peptides containing only a single ionizable residue for the DR*0401 case summarized in Table 1. In addition, it is obvious that complexes between CLIP peptides with P6 and P9 glutamic acid bound to DR*04 MHC II have a pH stability ratio significantly lower than the complexes formed between neutral CLIP peptides and DR*04. From these limited results, it is not possible to test a quantitative theory of how increasing numbers of buried carboxylates affect the pH stability ratio. One might expect the dissociation rate constant ($k = t_{1/2}^{-1} \ln 2$) of a peptide containing two carboxylates to be

$$k = \frac{K_A[H^+]k_A + K_B[H^+]k_B + k_c}{[(K_A + K_B + K_D[H^+])[H^+] + 1]} \tag{5}$$

where K_A and K_B are protonation equilibrium constants for sites A and B, respectively; and k_A and k_B are dissociation constants when sites A and B are protonated, respectively; and k_c is the dissociation rate constant for the species where sites A and B are deprotonated. K_D is the equilibrium constant for double protonation given by

$$K_D = [CH_2^{2+}]/([H^+]^2[C]) \tag{6}$$

where [C] is the concentration of the doubly deprotonated peptide. In this calculation, the dissociation rate constant of the doubly protonated species is set equal to zero. In the case where sites A and B are independent:

$$K_D = K_A K_B \tag{7}$$

As an example, assume that eq 7 is valid, $K_A = K_B = 10^{7.7}$ and that k_c dominates the numerator of eq 5. In this case, the pH ratio of a complex with a peptide with two ionizable residues is simply the product of the pH ratio of each complex with a peptide having a single ionizable residue. Only in the special case just described will additional buried ionizable residues on a peptide have a simple multiplicative effect on the pH ratio of the complex.

MODEL BUILDING

Two structures of the HCgp-39 327−337/HLA-DR4*0401 complex were modeled based on the crystal structure of a collagen II/DR*0401 complex (2). The two model structures were based on two molecular modeling approaches described in Materials and Methods. The degrees of burial of the various side chain peptide carboxylate groups (CO_2) were measured based on the burial option in the LOOK software. The calculated P2 Asp carboxylate percent burial values were 53% and 72%. The calculated P3 Asp carboxylate percent burial values were 90% and 92%. Finally, burial values of 40% and 82% were calculated for the P5 Glu carboxylate. Figure 4 summarizes the distribution of calculated burial values for all peptide carboxylate headgroups of the complexes listed in Table 1 as well as peptide carboxylate burial values for models of the hypothetical Invariant Chain CLIP/DR*0401 complexes where peptide positions 1 and 8 were substituted with Asp or Glu as indicated. However, percent burial and pH ratio differences between peptide aspartate and glutamate in peptide/MHC II complexes were not addressed comprehensively; therefore, our discussions are limited to the complexes studied experimentally. Clearly, peptide carboxylates at the P2, P5, P8 (especially Glu), and P10 pockets have access to at least one conformation with a relatively low degree of burial. In contrast, peptide carboxylates at other pockets have significantly higher degrees of burial. These results are qualitatively consistent with other modeling measurements where percent side chain burial of peptide side chains in three different peptide/MHC II crystal structures were studied (4). In this work, P2, P5, P8, and P10 peptide side chains were generally found to have the highest degree of solvent exposure relative to the other positions in the complex. These findings are also consistent with immunological studies of peptide/MHC II where peptide P2, P5, and P8 and to some extent C-terminal residues have been found to be important T-cell receptor contacts (31−34).
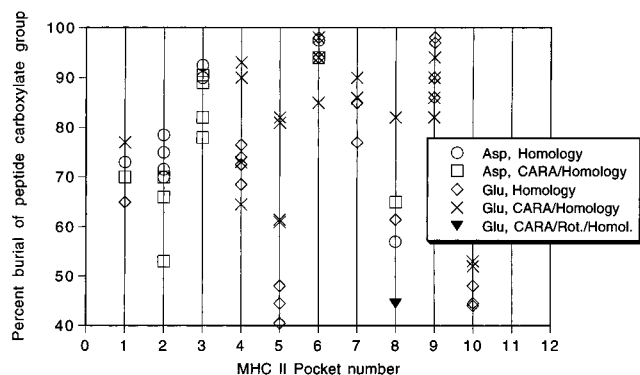
FIGURE 4: Burial of side-chain carboxylate groups. Percent burial values of peptide carboxylate groups from aspartic acid or glutamic acid placed at specified MHC II pocket positions in peptide/MHC II complexes listed in Table 1. Complexes between peptides with aspartic acid or glutamic acid placed at MHC II pocket positions 1 or 8 were not experimentally studied, but theoretical models of complexes between mouse invariant chain (Ii CLIP) substituted with aspartic or glutamic acid at these positions and HLA-DR4*0401 were modeled. The burial values for these carboxylate groups were measured and reported as well. As indicated in this figure, peptide/ MHC II structures were generated with two different modeling approaches described in Materials and Methods. In a special modeling case of the CLIP/DR*0401 complex with glutamic acid substituted at peptide position 8, an alternate and plausible geometry of the Glu side chain in an all trans conformation was manually introduced at a specified stage of the modeling (inverted solid triangle, see Materials and Methods) with a resulting low carboxylate burial value. The interpretation of these results is that, within the complexes studied, peptides with carboxylates at MHC II pocket positions P2, P5, P8, and P10 have a relaxed conformation with low carboxylate burial relative to the other pocket positions.

DISCUSSION

The majority of dissociation kinetics observed in the present study conform closely to single exponentials. Therefore we consider only two protein–peptide complexes: a protonated complex and a deprotonated complex. These complexes interconvert rapidly as compared to the rates of peptide dissociation; otherwise dissociations would be biphasic. The data supporting this interpretation of the kinetics are given in Figures 2 and 3. Rapid interconversion is also consistent with the sample preparation experiments mentioned earlier. On the basis of the kinetic scheme used for Figure 2, the path of dissociation is one in which only the deprotonated form of the complex dissociates at an appreciable rate, and the net rate of dissociation is a measure of the proportion of this deprotonated complex present under quasi-equilibrium conditions at a given pH. This effect is reflected by the unusual pH stability ratio in which the complex is much less stable at the higher pH. Mutations of the wild-type peptide f327–337 show that this unusual pH stability ratio is due to the aspartic acid residue 330 at the position of the P3 pocket. The two-state model in eq 1 is also supported by the studies of the desmoglein 3 f192–204/DR*0402 autoantigenic complex. It is likely that the rapid interconversion of protonated and deprotonated complexes applies also to the other peptide mutants listed in Table 1 (the model may fail if there are three isomers).

The pK_a values of the aspartate side chain in aqueous solution is about 3.9 (35). For a pK_a for the interconversion of the protonated and deprotonated complex of 7.7, the free energy shift is ∼8.75 kT. This shift is presumably due directly or indirectly to poor solvation of the carboxylate

group in the presence of protein. The carboxylate group would be poorly solvated and lack a counterion if buried in a neutral protein pocket. The high pK_a of f327–337/ DR*0401 P3 Asp reflects the necessity for a strong basic solution for removal of proton from the carboxylate group in an otherwise nonionic environment. Similar arguments apply for the f192–204 desmoglein 3/DR*0402 complex, where peptide Glu is buried in the P9 pocket of 0402, where an internal MHC II salt bridge already exists and no positive residue is free to form a salt bridge with the peptide. Previous protein studies have shown that protein environment influences the pK_a of carboxylate side chains, often leading to pK_a values that are quite different from 3.9 (36–38). For example, Glu 35 of lysozyme has an experimentally determined pK_a of 6.1 (36). Potentiometric studies of lysine 66 buried in the hydrophobic core of staphylococcal nuclease have shown that the pK_a of Lys 66 is shifted down to approximately 6.4 as compared to its fully solvated pK_a value of 10.4 (39). Recently, a pK_a of 8.8 was experimentally determined for a glutamic acid buried in the hydrophobic core of a staphylococcal nuclease V66E mutant using potentiometric methods (40). In this study, a chain of water molecules was shown to partially hydrate the buried glutamic acid (40).

With respect to relating molecular structure models to kinetics, our data are consistent with the assignment of HCgp-39 peptide side chains to HLA-DR4*0401 protein pockets as described in previous work (17, 41). In this assignment, a tyrosine residue is located in the hydrophobic P1 pocket. Modeling results of peptide carboxylate residues provides a tentative explanation why in the wild-type peptide aspartic acid 330 in the P3 pocket is the critical residue rather than aspartic acid in the P2 pocket in terms of leading to anomalous complex stability dependence in pH. That is, peptide Asp at P2 may adopt a relaxed conformation with a relatively high degree of solvent exposure compared to Asp at the P3 pocket. This unusual pH ratio effect is not unique to the P3 pocket. Aspartic acid carboxylate at the P6 pocket is highly buried (94–98% burial). The mutant f327–337 D330N S333D places an aspartic acid in this pocket, resulting in a low pH stability ratio.

With respect to other MHC II pockets we have observed that peptides with Asp or Glu at solvent-exposed positions have normal pH stability ratios. A normal pH stability ratio was also found for a case where a peptide Glu is buried in the P4 pocket of DR*0401. However, for most complexes with peptide carboxylates at relatively buried pockets a low pH stability ratio was observed. Placement of a peptide ionizable residue at a given pocket position in different MHC II alleles can lead to quite different pH stability ratios for the complexes as shown in Table 1. These results can be explained in terms of the potential for the peptide carboxylate to form a salt bridge with the MHC protein. For example, DR*0401 and 0404 (but not 0402) have a positively charged residue at position β 71 that has been hypothesized to form a salt bridge with peptide carboxylate residues in the P4 pocket. However, peptides with Asp or Glu at P4 are 20– 50-fold more stable bound to 0401 than to 0404 (42). This suggests that the salt bridge between peptide P4 Asp or Glu and DR*0401 is weak or not present in 0404. The complex between the peptide in Table 1 with Glu at P4 and DR*0404 has a moderately low pH stability ratio, consistent with a weak interaction between peptide P4 Glu residue and

DR*0404 β-Arg 71. In contrast, the pH stability ratio for peptides with Glu at P4 and DR*0401 is high, consistent with the presence of a strong peptide/DR*0401 salt bridge (see Table 1). Internal salt bridges reduce considerably the pK_a of carboxylic acid residues. For example, Asp 194 in α-chymotrypsin has a pK_a smaller than 2 and forms a buried salt bridge with the amino terminus Ile 16 (*36*). Similarly, Asp 102 and His 57 form an ion pair in serine proteases, shifting the pK_a of Asp below 2 (*37*). Therefore, the normal pH ratio of the human collagen II/0401 complex is consistent with the presence of a salt bridge. The P4 pocket of DR*04 alleles is of particular interest because the DR*0401 and DR*0404 MHC II alleles, but not the DR*0402 allele, are associated with susceptibility to RA (*42, 43*).

Complexes that are relatively short-lived at pH 7 might be expected to have reduced immunogenicity, since T cell receptor recognition usually occurs at this pH. By the same token, T cells specific for such complexes could escape thymic deletion. Indeed, in experimental autoimmune encephalomyelitis, a murine model of multiple sclerosis, an N-terminal peptide of myelin basic protein (MBP) is an immunodominant epitope (*14, 44–47*). The MBP peptide forms a short-lived complex with I–A^u with a half-life of 15 min (*47*). Supporting experiments have been reported where short half-lives of MBP/I–A^u complexes and other complexes allow escape from tolerance induction during early maturation of the organism (*14–16*).

Several scenarios may be envisioned in which T cells with specificity for such complexes could then become activated in the periphery. Under abnormal circumstances of high exogenous peptide concentration—where a large off rate for peptide dissociation at pH 7 would not limit cell surface complex concentration—such complexes might accumulate sufficiently to trigger a T cell response. Alternatively, peptide/MHC complexes with increased stability at acidic pH might also accumulate in pathologically induced acidic environments, such as the inflamed synovium, where local pH falls to below pH 6.5 (*48*). Evidence supporting the possibility that T cells reactive to complexes with unusual pH stability may play a role in autoimmunity is found in PV. PV is an autoimmune skin disease genetically linked to HLA-DR4*0402 allele (*20, 49–51*). The key autoantigen has been identified as desmoglein 3, and T cells recognizing the desmoglein 3 peptide 190–204 can be isolated from DR*0402 PV patients (*20*). As we have shown here, this peptide binds to DR*0402 in a register that places glutamic acid at the P9 pocket, which leads to a low pH ratio and a short half-life for the complex at pH 7.

In conclusion, it is interesting to note that the replacement of a carboxylic acid side chain by a neutral side chain has been used in connection with model vaccine development for melanoma. Tyrosinase is a transmembrane protein which is highly expressed by melanoma cells and has been shown to trigger an anti-melanoma immune response in human patients (*52*). Melanoma-specific T cells recognize wild-yype HLA-DR-restricted tyrosinase epitopes. Specifically, tyrosinase (Ty) 448–462 (DYS**Y**LQDSDPDSFQD) is recognized by certain T cells in the context of DR*0401, where the peptide was shown to bind with Y451 as the P1 anchor (shown in bold type) (*52*). This places Ty Asp 456 in the P6 pocket of DR*0401. Mutation of Asp 456 in this peptide to a neutral residue (Val) resulted in increased binding

affinity of the peptide to DR*0401 and ~1000-fold more potency in stimulating cytokine (GM-CSF) release from specific T cells (*52*). The Ty 448–462/DR*0401 complex most likely has a short half-life at neutral pH due to peptide burial of Asp 456 in the P6 pocket, and this is reflected in poor MHC II binding and T cell stimulation and in the failure of induction of tolerance to this self-epitope, which allows it to become antigenic when highly expressed by tumor cells.

ACKNOWLEDGMENT

REFERENCES

1. Abbas, A. K., Lichtman, A. H., and Pober, J. S. (1991) *Cellular and Molecular Immunology*, W. B. Saunders Company, Philadelphia.
2. Dessen, A., Lawrence, C. M., Cupo, S., Zaller, D. M., and Wiley, D. C. (1997) *Immunity 7*, 473–481.
3. Freemont, D. H., Hendrickson, W. A., Marrack, P., and Kappler, J. (1996) *Science 272*, 1001–1004.
4. Fremont, D. H., Monnaie, D., Nelson, C. A., Hendrickson, W. A., and Unanue, E. R. (1998) *Immunity 8*, 305–317.
5. Brown, J. H., Jardetzky, T. S., Gorga, J. C., Stern, L. J., Urban, R. G., Strominger, J. L., and Wiley, D. C. (1993) *Nature 364*, 33–39.
6. Sloan, V. S., Cameron, P., Porter, G., Gammon, M., Amaya, M., Mellins, E., and Zaller, D. M. (1995) *Nature 375*, 802–806.
7. Weber, D. A., Evavold, B. D., and Jensen, P. E. (1996) *Science 274*, 618–620.
8. Denzin, L. K., and Cresswell, P. (1995) *Cell 82*, 155–165.
9. Rabinowitz, J. D., Vrljic, M., Kasson, P. M., Liang, M. N., Busch, R., Boniface, J. J., Davis, M. M., and McConnell, H. M. (1998) *Immunity 9*, 699–709.
10. Hall, F. C., Rabinowitz, J. D., Belmares, M. P., Busch, R., Patil, N., Cope, A., Patel, S., Sonderstrup, G., Mellins, E. D., and McConnell, H. M. (2000) *J. Immunol.* (submitted).
11. Jensen, P. E. (1991) *J. Exp. Med. 174*, 1111–1120.
12. Hausmann, D. H. F., Yu, B., Hausmann, S., and Wucherpfennig, K. W. (1999) *J. Exp. Med. 189*, 1723–1733.
13. Reay, P. A., Wettstein, D. A., and Davis, M. M. (1992) *EMBO J. 11*, 2829–2839.
14. Fairchild, P. J., Wildgoose, R., Atherton, E., Webb, S., and Wraith, D. C. (1993) *Int. Immunol. 5*, 1151–1158.
15. Liu, G. Y., Fairchild, P. J., Smith, R. M., Prowle, J. R., Kioussis, D., and Wraith, D. C. (1995) *Immunity 3*, 407–415.
16. Joosten, I., Wauben, M. H. M., Holewijn, M. C., Reske, K., Pedersen, L. F., Rosenboom, C. F. P., Hensen, E. J., Van Eden, W., and Buus, S. (1994) *Int. Immunol. 6*, 751–759.
17. Verheijden, G. F., Rijnders, A. W., Bos, E., and Coenen-de Roo, C. J. (1997) *Arthritis Rheum. 40*, 1115–1125.
18. Nepom, G. T., and Erlich, H. (1991) *Annu. Rev. Immunol. 9*, 493–525.
19. Gregersen, P. K., Silver, J., and Winchester, R. J. (1987) *Arthritis Rheum. 30*, 1205–1213.
20. Wucherpfennig, K. W., Yu, B., Bhol, K., Monos, D. S., Argyris, E., Karr, R. W., Ahmed, A. R., and Strominger, J. L. (1995) *Proc. Natl. Acad. Sci. U.S.A. 92*, 11935–11939.
21. Gorga, J. C., Horejsi, V., Johnson, D. R., Raghupathy, R., and Strominger, J. L. (1987) *J. Biol. Chem. 262*, 16087–16094.
22. Busch, R., Reich, Z., Zaller, D. M., Sloan, V., and Mellins, E. D. (1998) *J. Biol. Chem. 273*, 27557–27564.
23. Schmitt, L., Boniface, J. J., Davis, M. M., and McConnell, H. M. (1998) *Biochemistry 37*, 17371–17380.
24. Levitt, M. (1983) *J. Mol. Biol. 170*, 723–764.
25. Levitt, M. (1992) *J. Mol. Biol. 226*, 507–33.
26. Lee, C., and Subbiah, S. (1991) *J. Mol. Biol. 217*, 373–388.

27. Lee, C. (1994) *J. Mol. Biol. 236*, 918−939.

28. Lee, C. (1996) *Fold Des. 1*, 1−12.

29. Chothia, C. (1976) *J. Mol. Biol. 105*, 1−14.

30. Hammer, J., Bono, E., Gallazzi, F., Belunis, C., Nagy, Z., and Sinigaglia, F. (1994) *J. Exp. Med. 180*, 2353−2358.

31. Allen, P. M., Matsueda, G. R., Evans, R. J., Dunbar, J. B. J., Marshall, G. R., and Unanue, E. R. (1987) *Nature 327*, 713−715.

32. Stern, L., Brown, G., Jardetzky, T., Gorga, J., Urban, R., Strominger, J., and Wiley, D. (1994) *Nature 368*, 215−221.

33. Reay, P. A., Kantor, R. M., and Davis, M. M. (1994) *J. Immunol. 152*, 3946−3957.

34. Carson, R. T., Vignali, K. M., Woodland, D. L., and Vignali, D. A. (1997) *Immunity 7*, 387−400.

35. Christopher, K., and van Holde, M. K. E. (1990) *Biochemisty*, 1st ed., Benjamin/Cummings Publishing Company, Redwood City, CA.

36. Antosiewicz, J., McCammon, A., and Gilson, M. K. (1994) *J. Mol. Biol. 238*, 415−436.

37. Yang, A., Gunner, R. M., Sampogna, R., Sharp, K., and Honig, B. (1993) *Proteins: Struct. Funct. Genet. 15*, 252−265.

38. Boniface, J. J., Allbritton, N. L., Reay, P. A., Kantor, R. M., Stryer, L., and Davis, M. M. (1993) *Biochemistry 32*, 11761−11768.

39. Garcia-Moreno E. B., Dwyer, J. J., Gittis, A. G., Lattman, E. E., Spencer, D. S., and Stites, W. E. (1997) *Biophys. Chem. 64*, 211−224.

40. Dwyer, J. J., Gittis, A. G., Karp, D., Lattman, E. E., Spencer, D. S., Stites, W. E., and Garcia-Moreno E., B. (2000) *Biophys. Chem.* (in press).

41. Marshall, K. W., Wilson, K. J., Liang, J., Woods, A., Zaller, D., and Rothbard, J. B. (1995) *J. Immunol. 154*, 5927−5933.

42. Hammer, J., Gallazi, F., Bono, E., Karr, R. W., Guenot, J., Valsasnini, P., Nagy, Z. A., and Sinigaglia, F. (1995) *J. Exp. Med. 181*, 1847−1855.

43. Woulfe, S. L., Bono, C. P., Zacheis, M. L., Kirschmann, D. A., Baudino, T. A., Swearingen, C., Karr, R. W., and Schwartz, B. D. (1995) *Arthritis Rheum. 38*, 1744−1753.

44. Wraith, D. C., Smilek, D. E., Mitchell, D. J., Steinman, L., and McDevitt, H. O. (1989) *Cell 59*, 247−255.

45. Gautam, A. M., Lock, C. B., Smilek, D. E., Pearson, C. I., Steinman, L., and McDevitt, H. O. (1994) *Proc. Natl. Acad. Sci. U.S.A. 91*, 767−771.

46. Smilek, D. E., Wraith, D. C., Hodgkinson, S., Dwivedy, S., Steinman, L., and McDevitt, H. O. (1991) *Proc. Natl. Acad. Sci. U.S.A. 88*, 9633−9637.

47. Lee, C., Liang, M. N., Tate, K. M., Rabinowitz, J. D., Beeson, C., Jones, P. P., and McConnell, H. M. (1998) *J. Exp. Med. 187*, 1505−1516.

48. Halliwell, B., Gutteridge, J. M., and Blake, D. (1985) *Philos. Trans. R. Soc. London, Ser. B 311*, 659−671.

49. Ahmed, A. R., Yunis, E. J., Khatri, K., Wagner, R., Notani, G., Awdeh, Z., and Alper, C. A. (1990) *Proc. Natl. Acad. Sci. U.S.A. 87*, 7658−7662.

50. Scharf, S. J., Friedmann, A., Brautbar, C., Szafer, F., Steinman, L., Horn, G., Gyllensten, U., and Erlich, H. A. (1988) *Proc. Natl. Acad. Sci. U.S.A. 85*, 3504−3508.

51. Scharf, S. J., Long, C. M., and Erlich, H. A. (1988) *Hum. Immunol. 22*, 61−69.

52. Topalian, S. L., Gonzales, M. I., Parkhurst, M., Li, Y. F., Southwood, S., Sette, A., Rosenberg, S. A., and Robbins, P. F. (1996) *J. Exp. Med. 183*, 1965−1971.